














ORIGINAL RESEARCH ARTICLE

Adducin Regulates Sarcomere Disassembly During Cardiomyocyte Mitosis

Feng Xiao, PhD*¹; Ngoc Uyen Nhi Nguyen , PhD*²; Ping Wang, PhD³; Shujuan Li, MD, PhD⁴; Ching-Cheng Hsu, PhD⁵; Suwannee Thet, MS⁶; Wataru Kimura , PhD⁷; Xiang Luo , MD, PhD⁸; Nicholas T. Lam, PhD⁹; Ivan Menendez-Montes, PhD¹⁰; Waleed Elhelaly , MD, PhD¹¹; Alisson Campos Cardoso , PhD¹²; Ana Helena Macedo Pereira, PhD¹³; Rohit Singh, PhD¹⁴; Sakthivel Sadayappan , PhD¹⁵; Mohammed Kanchwala , PhD¹⁶; Chao Xing , PhD¹⁷; Feria A. Ladha , PhD¹⁸; J. Travis Hinson , MD¹⁹; Roger J. Hajjar , MD²⁰; Joseph A. Hill , MD, PhD²¹; Hesham A. Sadek , MD, PhD²²

BACKGROUND: Recent interest in understanding cardiomyocyte cell cycle has been driven by potential therapeutic applications in cardiomyopathy. However, despite recent advances, cardiomyocyte mitosis remains a poorly understood process. For example, it is unclear how sarcomeres are disassembled during mitosis to allow the abscission of daughter cardiomyocytes.

METHODS: Here, we use a proteomics screen to identify adducin, an actin capping protein previously not studied in cardiomyocytes, as a regulator of sarcomere disassembly. We generated many adeno-associated viruses and cardiomyocyte-specific genetic gain-of-function models to examine the role of adducin in neonatal and adult cardiomyocytes in vitro and in vivo.

RESULTS: We identify adducin as a regulator of sarcomere disassembly during mammalian cardiomyocyte mitosis. α/γ -adducins are selectively expressed in neonatal mitotic cardiomyocytes, and their levels decline precipitously thereafter. Cardiomyocyte-specific overexpression of various splice isoforms and phospho-isoforms of α -adducin in identified Thr445/Thr480 phosphorylation of a short isoform of α -adducin as a potent inducer of neonatal cardiomyocyte sarcomere disassembly. Concomitant overexpression of this α -adducin variant along with γ -adducin resulted in stabilization of the adducin complex and persistent sarcomere disassembly in adult mice, which is mediated by interaction with α -actinin.

CONCLUSIONS: These results highlight an important mechanism for coordinating cytoskeletal morphological changes during cardiomyocyte mitosis.

Key Words: α -actinin ■ adducin ■ cardiac proliferation ■ Irak4 ■ sarcomere disassembly

Cardiomyocyte loss is a leading cause of heart failure, which is a devastating progressive disease affecting >30 million patients worldwide.¹ Although limited cardiomyocyte renewal occurs in the adult mammalian heart, it is insufficient for restoration of contractile function after cardiomyocyte loss, which results in cardiomyopathy.²⁻⁷ Therefore, stimulating cardiomyocyte regeneration is a major goal of heart repair

in cardiomyopathy. Unlike some lower vertebrates that possess a lifelong cardiac regeneration capacity,⁸⁻¹⁴ adult mammalian cardiomyocytes permanently withdraw from the cell cycle shortly after birth and have a very limited regenerative potential. Studies in neonatal mouse hearts showed that apical resection or myocardial infarction (MI) of postnatal day 1 (P1) mice leads to a robust regenerative response; however, this capacity is lost by

Correspondence to: Hesham A. Sadek, MD, PhD, Departments of Internal Medicine/Cardiology, University of Texas Southwestern Medical Center, 6000 Harry Hines Blvd, Dallas, TX 75390. Email hesham.sadek@utsouthwestern.edu

This manuscript was sent to Ju Chen, MD, Guest Editor, for review by expert referees, editorial decision, and final disposition.

*F.X. and N.U.N.N. contributed equally.

Supplemental Material is available at <https://www.ahajournals.org/doi/suppl/10.1161/CIRCULATIONAHA.122.059102>.

For Sources of Funding and Disclosures, see page XXX.

© 2024 American Heart Association, Inc.

Circulation is available at www.ahajournals.org/journal/circ

Clinical Perspective

What Is New?

- Mammalian hearts can regenerate spontaneously in the first few days of life but lose this ability as cardiomyocytes stop dividing shortly after birth. Sarcomere disassembly during mitosis is crucial for this early heart regeneration.
- Here, we identify adducin, a protein previously not studied in the heart, as a critical regulator of sarcomere disassembly during cardiomyocyte mitosis. Forced expressions of adducin in adult hearts result in sarcomere disassembly and increased cardiomyocyte mitosis.
- Adducin induces sarcomere disassembly by interacting with α -actinin.

What Are the Clinical Implications?

- These results identify adducin as a regulator of sarcomere disassembly during cardiomyocyte mitosis during mammalian neonatal heart regeneration.
- Modulating adducin expression promotes sarcomere disassembly and enhances the regenerative capacity of adult cardiomyocytes.
- These findings indicate that targeting sarcomere disassembly is plausible therapeutic strategy to promote myocardial regeneration.

P7, which coincides with postnatal cardiomyocyte cell cycle arrest.^{15,16} Although several regulators of the cardiomyocyte cell cycle have been identified,^{17–23} it is not clear whether there are cytoskeletal-specific factors that regulate mitosis in cardiomyocytes.

The dense myofibrillar composition of cardiomyocytes poses a special challenge during mitosis, which is a consideration that does not exist in other nonstriated cells. In an adult cardiomyocyte, sarcomeres occupy >60% of cardiomyocyte cytoplasm²⁴ and anchor to the plasma membrane to induce deformation of the cell during contraction. An important and interesting feature of regenerating hearts is the disassembly of cardiomyocyte sarcomeres^{15,25,26} and their peripheral marginalization during cardiomyocyte mitosis (Figure 1A).²⁷ This phenomenon has long been observed in dividing cardiomyocytes and has proven to be a reliable indicator of cardiomyocyte mitosis in the early postnatal heart.^{15,17,22,28} However, to date, the mechanisms that regulate sarcomere disassembly are not understood. Moreover, it is unclear whether the regulation of sarcomere disassembly plays a role in the loss of the regenerative capacity of the neonatal heart with advancing postnatal age. In the current study, we set out to identify regulators of cardiomyocyte sarcomere disassembly during mitosis. We found that the cytoskeletal regulatory protein adducin is a critical regulator of sarcomere disassembly.

Nonstandard Abbreviations and Acronyms

α-MHC	α -myosin heavy chain
AAV	adeno-associated virus
Actn2	α -actinin
Add1	α -adducin
Add1_i1	full-length Add1 isoform 1 (long form)
Add1_i2	Add1 isoform 2 (short form)
Add1_pT445	phosphorylation at Add1_threonine 445 and 480 (T445/T480)
Add3	γ -adducin
Cas9	CRISPR-associated protein 9
CDK1	cyclin-dependent kinase 1
Co-IP	coimmunoprecipitation
CRISPR	Clustered regularly interspaced short palindromic repeats
Dcamk12	doublecortin-like and CAM kinase-like 2
dTG	double transgenic
GFP	green fluorescent protein
HW/BW	heart weight to body weight ratio
Irak4	interleukin 1 receptor associated kinase 4
LV	left ventricular
MI	myocardial infarction
Nek1	NIMA-related kinase 1
NRVM	neonatal rat ventricle myocyte
P	postnatal day
p-dTG	phospho-double transgenic
pH3	phospho-histone H3-Ser10
PKA	protein kinase A
PKC	protein kinase C
PLA	proximity ligation assay
S	serine
T	threonine
TG	transgenic
Tnnt2	cardiac troponin T
TUNEL	TdT-mediated dUTP nick end labeling
WB	Western blot
WT	wild-type

METHODS

Detailed descriptions of materials and methods and information on statistical tests are provided in the [Supplemental Material](#). All data and methods used in this analysis will be made available to researchers upon request. The use of animals in this study was approved by the institutional animal care and use committee of the University of Texas Southwestern Medical Center. Experimental analysis was performed in a double-blind fashion. Statistical analysis and plotting were performed using

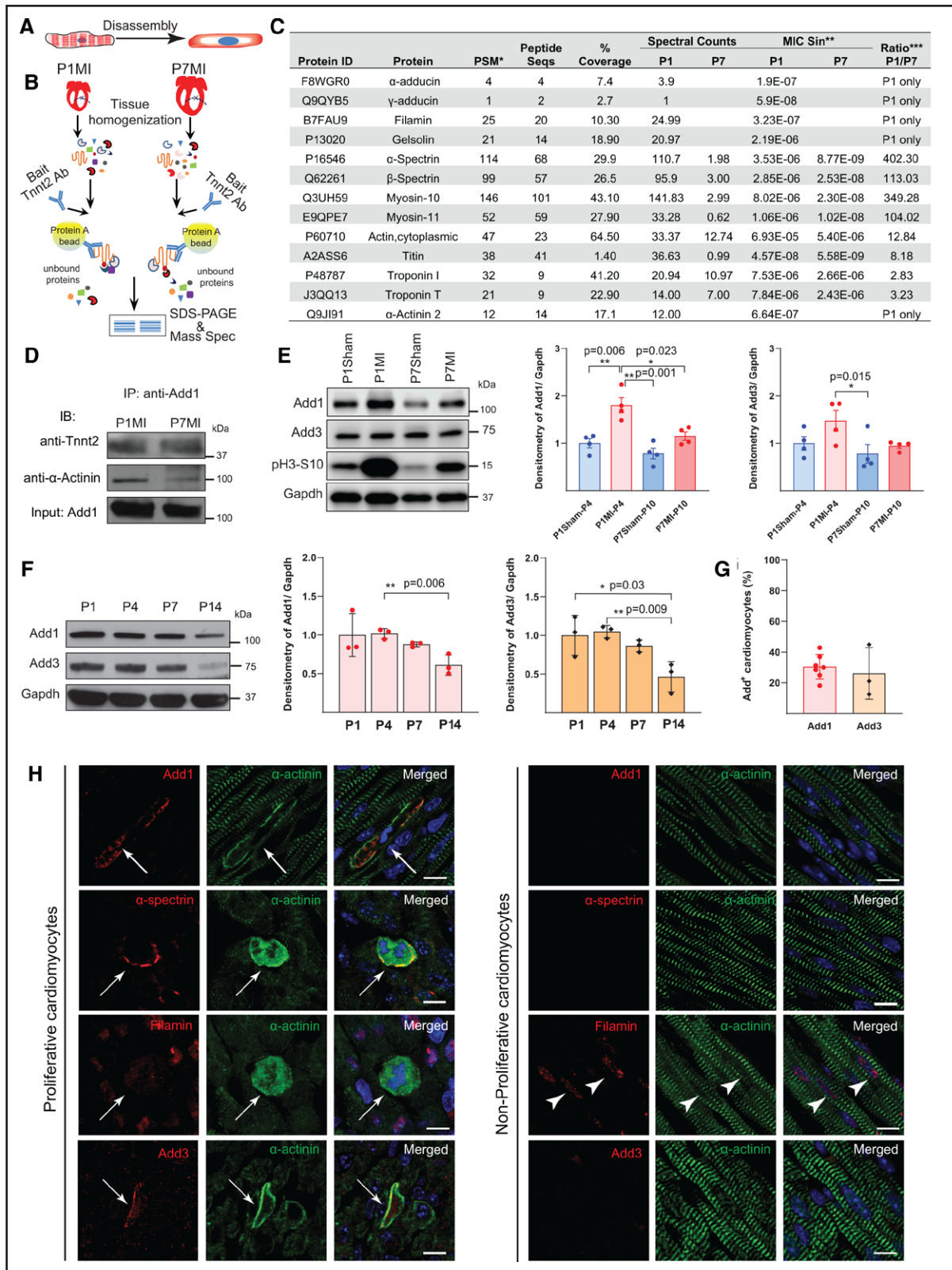


Figure 1. Identification of Adducin as a key protein associated with sarcomere disassembly and cardiomyocyte proliferation.

A, Schematic representation of sarcomere disassembly morphology. **B**, Coimmunoprecipitation (Co-IP) coupled with mass spectrometry (MS) workflow, using Tntt2 pulldown to identify associated proteins from total heart extracts 3 days after myocardial infarction (MI) at postnatal day 1 (P1MI) and P7 (P7MI). **C**, Table summarizing key proteins associated with Tntt2, as identified from Co-IP/MS. *Peptide spectrum matches (PSM) indicates the number of spectra assigned to peptides that contributed to the inference of the protein. **MIC Sin represents the normalized spectral index statistic for each protein, calculated from the intensity of fragment ions in each spectrum assigned to a protein. ***Ratio between (Continued)

Figure 1 Continued. groups derived from MIC Sin values. **D**, Co-IP of Add1 from P1MI and P7MI, probed for Tnnt2 and α -actinin. **E, Left**, Representative Western blot (WB). **Right**, Quantitative comparison of Add1 and Add3 protein expression at 3 days after sham surgery or MI at P1 and P7. The pH3-S10 is included as a biomarker to indicate the occurrence of MI. **F, Left**, Representative WB. **Right**, Quantification of endogenous expression of Add1 and Add3 at different postnatal ages. Gapdh serves as a loading control in **E** and **F**. **G**, Percentage of cardiomyocytes expressing adducins in neonatal hearts. **H**, Immunostaining for selected cytoskeletal proteins (Add1, Add3, spectrin, filamin) in proliferative (**left**) and nonproliferative (**right**) neonatal cardiomyocytes. Arrows indicate proliferative cardiomyocytes. Arrowheads in filamin staining refers to the nucleus location. Scale bar=10 μ m (**H**). Data are presented as mean \pm SD. Statistical analyses: 2-way ANOVA with Tukey post hoc test (**E**), and Kruskal-Wallis with uncorrected Dunn test (**F**); * P <0.05; ** P <0.01.

GraphPad Prism (v.10.1.0; GraphPad Software Inc, San Diego, CA). Data were tested for normality before parametric statistics were applied using the Kolmogorov-Smirnov test. Data were analyzed by the 2-tailed Mann-Whitney U test or the 2-tailed Student unpaired t test to compare means when there were 2 experimental groups, by Kruskal-Wallis with uncorrected Dunn test or 1-way ANOVA followed by Tukey post hoc test to compare means among ≥ 3 groups, or by 2-way ANOVA to compare means when there were ≥ 2 independent variables. Differences between the groups were considered significant at P <0.05.

RESULTS

Adducin Is Highly Expressed in Neonatal Regeneration, Closely Associated With Disassembled Sarcomeres

In our previous studies, immunostaining of Tnnt2 (cardiac troponin T), a crucial sarcomere protein, revealed a pivotal process related to the neonatal cardiomyocyte proliferation: sarcomere disassembly and relocation to the submembranous area in mitotic cardiomyocytes.¹⁵ This presence of Tnnt2 in disassembled sarcomeres can thus be used to further explore novel disassembly-regulated proteins. Using mass spectrometry after coimmunoprecipitation (Co-IP) with a Tnnt2 antibody, we examined Tnnt2-associated proteomes at 2 stages: 3 days after MI in day-1 (P1MI) and day-7 (P7MI) postnatal hearts, correlating to high and low cardiomyocyte mitosis and disassembly activities, respectively (Figure 1B). Our findings showed a significant cytoskeletal protein presence (Table S1), highlighting the differential association of Add1 (α -adducin) and Add3 (γ -adducin) with Tnnt2 during the regenerative window (Figure 1C). Although detected at lower levels, both adducins were identified exclusively in the P1MI samples, not unlike α -actinin. Spectrin, a well-known adducin-interacting protein, also predominantly interacted with Tnnt2 in the P1MI but less expressed in P7MI (Figure 1C). Reverse Co-IP using Add1 antibody as a bait in P1MI and P7MI hearts confirmed the interaction of Add1 with Tnnt2 and also its strong association with α -actinin in P1MI hearts (Figure 1D). These results suggest the relevance of adducin presence and cardiomyocyte proliferation.

We further examined the relationship between adducin expression and cardiomyocyte proliferation using Western blot (WB). After P1MI, a period of intense proliferation marked by high levels of the mitotic marker

phospho-histone H3-Ser10 (pH3), Add1 expression significantly increased compared with P1Sham. In contrast, P7MI hearts displayed a marginal, nonsignificant increase in adducin expression compared with P7Sham. Add3 levels remained unchanged between MI and Sham groups (Figure 1E). Additionally, both Add1 and Add3 showed decreased expression with increasing postnatal age (Figure 1F). Therefore, we assessed whether the Add1-Tnnt2 interaction aligns more with robust cardiomyocyte proliferation than maturation. We conducted Co-IP using adducin or Tnnt2 antibodies as baits on P1MI or sham surgery neonatal hearts (Figure S1A and S1B). The results confirmed a stronger Add1-Tnnt2 interaction in higher proliferation status P1MI (Figure S1C and S1D). We noted a mild but noticeable Add1-Tnnt2 interaction in P1Sham, attributable to the ongoing cardiomyocyte proliferation at this stage (Figure S1C and S1D). Conversely, to confirm adducin capability in stimulating cardiomyocyte mitosis, we knocked down Add1 and Add3 in neonatal rat ventricle myocytes (NRVM) through siRNA and monitored proliferation through pH3 staining (Figure S2A). WB confirmed the successful knockdown, particularly with tandem siRNA targeting both Add1 and Add3 (Figure S2B). siRNA-mediated adducin knockdown led to reduced mitotic rates (Figure S2C), underlining their importance in neonatal cardiomyocyte proliferation.

Immunohistochemistry revealed adducin expression in $\approx 30\%$ of neonatal cardiomyocytes (Figure 1G), with Add1, Add3, and spectrin specifically associated with disassembled sarcomeres in proliferating cells, localizing in the membranous and submembranous areas (Figure 1H). Conversely, α -filamin displayed a nuclear staining pattern in nonproliferating cells and a diffuse cytoplasmic pattern in proliferating cardiomyocytes. siRNA-mediated Add1 and Add3 loss led to a decline in sarcomere disassembly rates (Figure S2D). These observations reinforce the role of adducin in sarcomere disassembly during cardiomyocyte proliferation in the neonatal heart.

Overexpression of Add1 Isoform 2 Results in Transient Disassembly of Sarcomeres

Alternative splicing plays an important role in heart development and cardiomyopathies, significantly affecting posttranscriptional regulation.^{29–33} Although previous studies focused on the full-length Add1 isoform 1

(Add1_i1), there is another major isoform, Add1 isoform 2 (Add1_i2), differentiated by the exclusion of exon 15 (Figure 2A). Add1_i2, the shorter isoform lacking ≈ 100 amino acids at the C terminus, also declines in expression with postnatal age in mouse hearts, as observed in Add1_i1 (Figure 2B).

To explore the impact of Add1 on sarcomere disassembly, we infected NRVMs with either Add1_i1 or Add1_i2 using adeno-associated virus (AAV) 6, with AAV6-GFP (green fluorescent protein) serving as control. We categorized sarcomere disassembly into 3 patterns: assembled, partially disassembled, and fully disassembled. Partially disassembled sarcomeres, identifiable by α -actinin staining in red, contain some visible cytoplasmic sarcomeres (Figure 2Ci and 2Ciii), whereas fully disassembled sarcomeres lack them completely (Figure 2Cii and 2Civ). Overexpression of Add1_i1 resulted in 10.8% of cells with fully disassembled sarcomeres, whereas Add1_i2 led to 49.6% (Figure 2D). In contrast, GFP-infected NRVMs showed no sarcomere disassembly (Figure 2Cv). These results suggest that Add1_i2 overexpression led to a higher rate of complete sarcomere disassembly compared with Add1_i1.

Furthermore, we generated a cardiac-specific transgenic (TG) mouse model expressing Add1_i2 under an α -MHC (α -myosin heavy chain) promoter (Figure 2E). The *Add1_i2* TG mice exhibited no significant differences in cardiac size, morphology as indicated by hematoxylin and eosin (H&E) staining (Figure 2F), or heart weight to body weight ratio (HW/BW; Figure 2G). Postnatal analysis of these mice revealed a notable decrease in Add1-positive cardiomyocytes at P28 compared with P14 hearts (Figure 2H and 2I). It is important to note that at P14, *Add1_i2* TG displayed a significant increase in sarcomere disassembly, evidenced by reduced assembly scores (Figure 2J and 2K) and increased pH3⁺ cardiomyocytes (Figure S3A), without any change in cardiomyocyte size (Figure S3B). However, by P28, alongside a decrease in Add1_i2 expression, these hearts showed no significant change in assembly scores (Figure 2J and 2K) or left ventricular (LV) systolic function, assessed by echocardiography (Figure S3C), compared with wild-type (WT) mice. These results suggest that cardiomyocyte-specific overexpression of Add1_i2 results in a transient increase in sarcomere disassembly, which does not continue into adulthood.

Add1_Threonine 445 and 480 Phosphorylation Extends Neonatal Cardiomyocyte Sarcomere Disassembly

We explored the role of adducin phosphorylation in cardiomyocyte sarcomere disassembly by examining its phospho-isoforms expression in neonatal mouse hearts (Figure 3A). Studies indicate that phosphorylation at Add1_threonine (T) 445 and 480 (T445/T480) sites

enhances spectrin recruitment to F-actin.³⁴ We found Add1_pT445 at the cellular cortex in myocytes with disassembled sarcomeres and in the nuclei of nonproliferating cardiomyocytes (Figure 3A). In addition, phosphorylation by CDK1 (cyclin-dependent kinase 1) at serine (S) 12 and Ser355 associates Add1 with mitotic spindles,³⁵ and we noted Add1_pS355 localization in the cytoplasm of mitotic cardiomyocytes (Figure 3A). Add1 also has PKA (protein kinase A) and PKC phosphorylation sites at Ser716 and Ser726 (S714 and S724 in mice), Ser408, Ser436, and Ser481, which inhibit spectrin-F-actin binding.^{36,37} However, our study found no phosphorylation at S724 or S481 in neonatal cardiomyocytes (Figure 3A).

Furthermore, we correlated phospho-adducin expression with cardiomyocyte mitosis in vitro (Figure 3B) and in vivo (Figure S4A) using immunofluorescent staining. Add1_pT445 transitions from nuclear during prophase to cytoplasmic and mitotic chromosome-associated in metaphase with sarcomere disassembly initiation, and remains cytoplasmic through telophase. WB analysis showed that Add1_pT445 expression decreases with age, paralleling Add1 (Figure 3C). These results suggest that phosphorylation of Add1 at T445 and T480 might play a significant role in sarcomere disassembly during cardiomyocyte mitosis.

To determine whether Add1 phosphorylation at T445/T480 regulates cardiomyocyte sarcomere disassembly, we generated Add1 mutants mimicking phosphorylated (phospho-mimic) and nonphosphorylated (phospho-silent) states. We produced these variants using glutamic acid for the phospho-mimic and alanine for the phospho-silent forms with recombinant AAV6. We analyzed sarcomere morphology in NRVMs by staining with α -actinin antibody and identifying Add1-expressed cells as FLAG-positive. Our results indicated that nearly 60% of cells overexpressing the phospho-mimic Add1(T445E/T480E) showed complete sarcomere disassembly, whereas those with the phospho-silent form Add1(T445A/T480A) mostly exhibited partial disassembly (Figure 3D and 3E). Mutants for other phosphorylation sites (S12/S355 and S714/S724) were also tested but did not show a significant effect on complete disassembly (Figure S4B and S4C). These results led us to focus on the T445/T480 sites for their prominent role in sarcomere disassembly.

To determine whether forced expression of phospho-mimic Add1(T445E/T480E) induces sarcomere disassembly in cardiomyocytes in vivo, we developed an inducible cardiac-specific TG by breeding pTRE-Add1(T445E/T480E) with α MHC-tTA mice. This line expresses phospho-mimic Add1(T445E/T480E) in cardiomyocytes in the absence of doxycycline (Tet-off system) (Figure 3F). These mice showed no significant changes in heart morphology (Figure 3G) or HW/BW (Figure 3H) at P28. However, at P14, cardiomyocytes

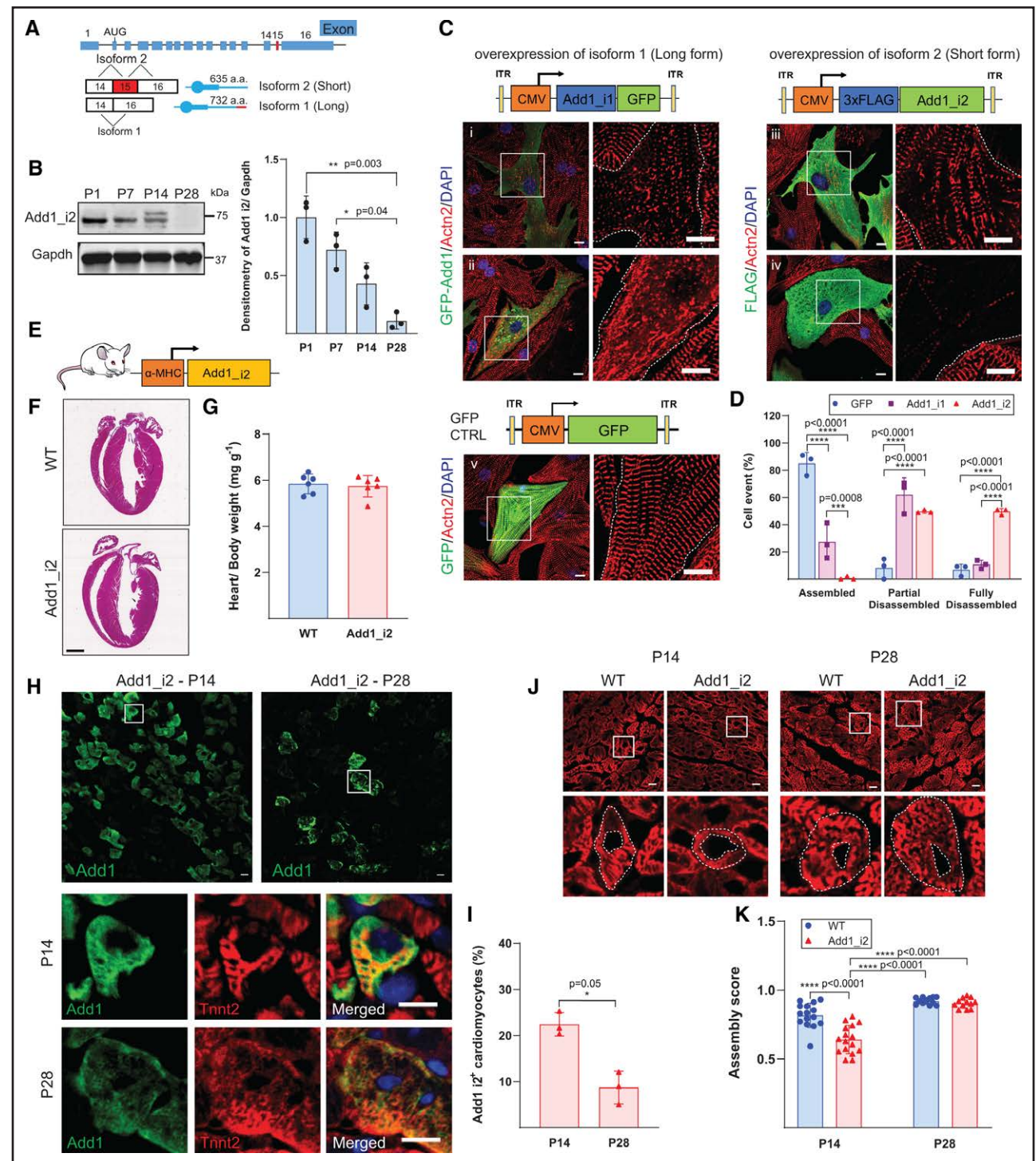


Figure 2. Overexpression of Add1 isoform 2 disassembles cardiomyocyte sarcomeres.

A, Top, Schematic detailing the exon-intron structure of the *Add1* gene. The red rectangle highlights exon15, the alternative splicing target. **Bottom**, Alternative splicing of exon15 in mRNA: inclusion results in Add1_i2 with 636 amino acids, whereas exclusion produces Add1_i1 with 732 amino acids. The corresponding protein schematics are displayed alongside. **B, Left**, Representative Western blot (WB). **Right**, Quantitative comparison of Add1_i2 endogenous expression across different ages, with Gapdh as an internal control. **C**, Representative images of NRVMs transfected with AAV6 viral particles for Add1_i1, Add1_i2, and GFP (green fluorescent protein) control at day 3. Cells were immunostained with α -actinin (Actn2, red) to visualize sarcomere structure. Green fluorescence indicates Add1_i1, Add1_i2, or GFP expression. High-magnification views of selected areas are shown to the right, depicting varying states of sarcomere assembly: **i** and **iii**, partially disassembled sarcomeres; **ii** and **iv**, fully disassembled sarcomeres; **v**, assembled sarcomeres. Dotted lines mark cardiomyocyte borders. **D**, Percentage of sarcomere disassembly in response to adducin overexpression in **C**. **E**, Generation strategy for Add1_i2 transgenic mice. **F**, Hematoxylin and eosin staining of wild-type (WT) and Add1_i2 transgenic hearts. **G**, HW/BW comparison in control and Add1_i2 transgenic mice. **H, Top**, Images showing Add1_i2 expression patterns in transgenic mice at postnatal day 14 (P14) and P28. **Bottom**, Insets show enlarged views of individual (Continued)

Figure 2 Continued. cardiomyocytes. **I**, Proportion of cardiomyocytes expressing Add1_i2 in transgenic mice. **J, Top**, Images representing sarcomere patterns in *Add1_i2* transgenic mice at P14 and P28. **Bottom**, Insets show enlarged views of individual cardiomyocytes. Dotted lines indicate the outer and inner borders of sarcomeres. **K**, Comparisons of sarcomere disassembly scored with age-matched WT littermates indicate significant sarcomere thinning and central clearance in *Add1_i2* transgenic mice at P14. Scale bar=10 μ m (**C, H, and J**); scale bar=1 mm (**F**). Data are presented as mean \pm SD. Statistical analyses: Kruskal-Wallis with uncorrected Dunn test (**B**), Mann-Whitney *U* test (2-tailed; **I**), 2-way ANOVA with Tukey post hoc test (**D** and **K**; * P <0.05, ** P <0.01, *** P <0.001, and **** P <0.0001.

expressing the phospho-mimic Add1 displayed Add1 cytoplasmic localization and sarcomere disassembly, as evidenced by gaps in Tnnt2 and nucleus staining (Figure 3I). This disassembly was not evident at P28, with decreased Add1(T445E/T480E) (Figure 3I and 3J) and cardiomyocyte morphology returning to normal (Figure 3K and 3L). In addition, lack of significant differences in proliferation rate (Figure S5A) or cardiomyocyte size (Figure S5B) support the notion that phospho-mimic Add1 overexpression temporarily enhances sarcomere disassembly during early development, but this effect is not sustained to adulthood, not unlike *Add1_i2* TG line.

Concomitant Expression of Add1 and Add3 Is Required for Protein Stabilization

Previous research focused on Add1 because of its role in dimer formation with other adducin isoforms. Add1 knockout models indicated a reduction in Add3 expression. We observed that sarcomere disassembly in *Add1* TG lines was impaired after P14, coinciding with diminished endogenous Add3 expression by this age. This result suggests that the reduced disassembly capacity of *Add1* TG lines beyond P14 might be a result of the loss of Add3. To explore the interplay between Add1 and Add3, we conducted in vitro transfections using *Add1_i1* and *i2*, both with and without *Add3*. To avoid cross-reactivity between adducin isoforms, Add1 variants were tagged with FLAG, whereas Add3 variants were tagged with TY1. Cells were treated with 80 μ M cycloheximide 24 hours after transfection to inhibit protein synthesis and collected at various intervals thereafter. WB analysis showed that Add1 levels decreased over time in the absence of Add3. Conversely, in the presence of Add3, the levels of Add_i1 and i2 were maintained and ended up higher than those of Add1 alone at later time points (Figure 4A). These results suggest that the limited sarcomere disassembly observed in single *Add1* TG lines beyond P14 might be related to the absence of endogenous Add3 at later developmental stages.

Add1/Add3 Double Transgenic Mouse Model Exhibits Partial Sarcomere Disassembly in Adult Hearts

We generated cardiac-specific double transgenic (dTG) mouse line those coexpresses both *Add1_i2* and *Add3* (Figure 4B) to investigate their involvement in disassembly. Immunostaining confirmed the coexpression and co-

localization of these isoforms in cardiomyocytes (Figure S6A). To further understand the expression dynamics, we divided dTG mice into low and high *Add1_i2* mRNA expression groups (Figure 4C and 4G, respectively). *Add1_i2* endogenous expression is low after P14, making transgenic mRNA expression levels seem too high in comparison to the WT.

The low expression group showed normal cardiac morphology and HW/BW at 2 months old (Figure 4D) but slightly reduced LV systolic function (Figure 4E) compared with WT. Intriguingly, in cardiomyocytes where adducin was overexpressed, we observed partial sarcomere disassembly characterized by disorganized sarcomeres lacking clear striations (Figure 4F). However, the typical pattern of complete sarcomere disassembly and clearance was not evident.

The high expression group had about double the Add1 mRNA level of the low expression group (Figure 4G) and exhibited ventricular dilation (Figure 4H, left), increased HW/BW (Figure 4H, right), and markedly reduced LV systolic function (Figure 4I) at 2 months old. Partial sarcomere disassembly with focal localization of Tnnt2 to the intercalated disk was observed (Figure 4J), although some myocytes appeared with no significant sarcomere disorganization (Figure 4J, lower row). In addition, these mice also showed cardiomyocyte disruption and signs of increased cell death (Figure 4K), confirmed by TdT-mediated dUTP nick end labeling (TUNEL) assay (Figure S6B). Cardiomyocyte size analysis indicated a higher proportion of smaller cells in the high expression group (Figure S6C). These findings suggest that Add3 and Add1 coexpression stabilizes the adducin complex, leading to partial sarcomere disassembly, with the high expression group also experiencing cardiomyocyte death and diminished heart function.

Phospho-Mimic Add1/Add3 Double Transgenic Mouse Sustains Sarcomere Disassembly

The transgenic mouse expressing a phospho-mimic Add1(T445E/T480E) showed neonatal sarcomere disassembly, but not in adults (Figure 3G), likely because of reduced Add3 expression. To investigate further, we developed a phospho-double transgenic (p-dTG) mouse line coexpressing phospho-mimic *Add1_i2*(T445E/T480E) and WT-Add3 (Figure 5A, top). These mice had larger hearts as indicated by hematoxylin and eosin staining (Figure 5A, bottom) and a trend of increasing HW/BW (Figure 5B), with slightly lower LV ejection fraction

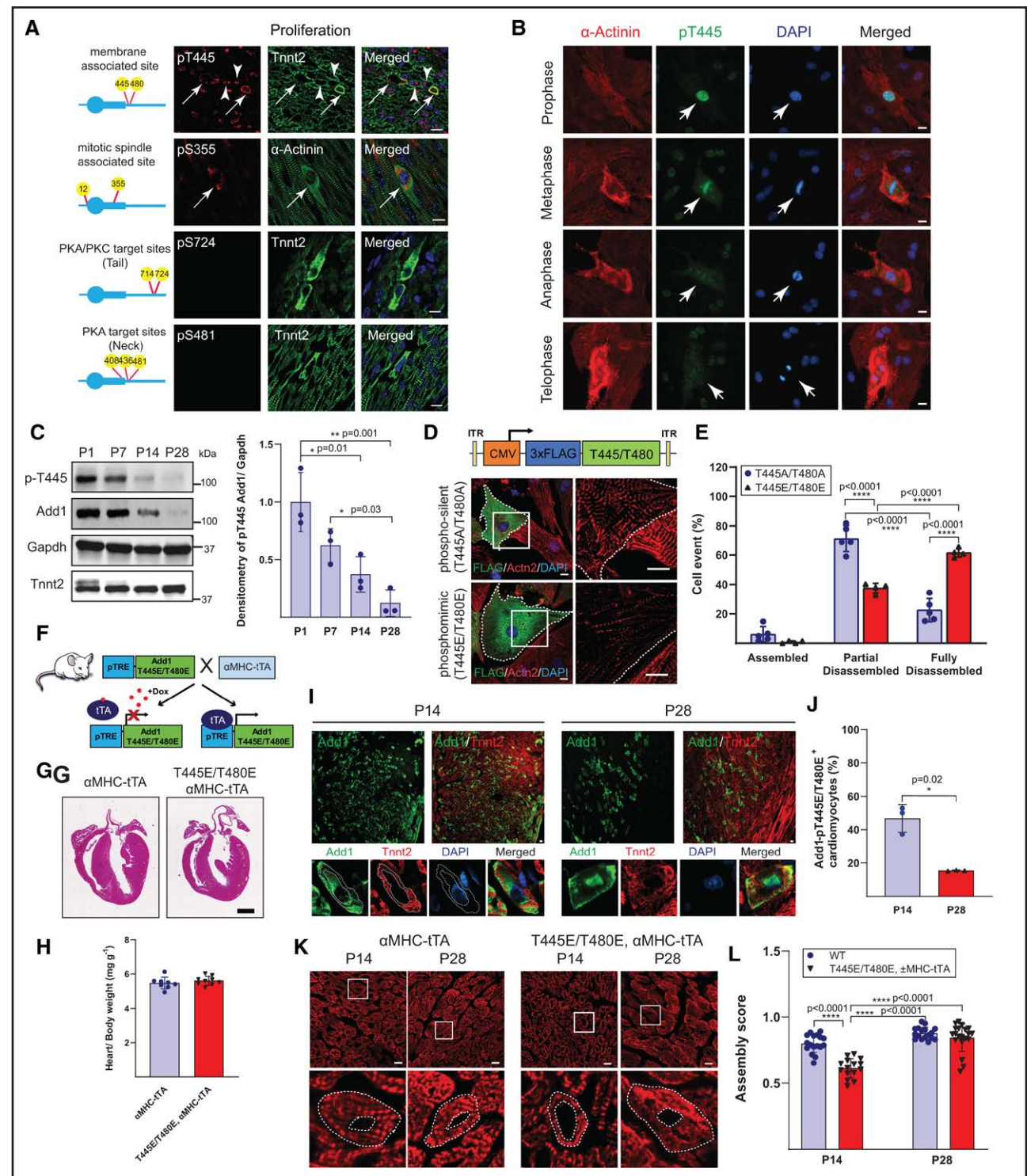


Figure 3. Role of Add1_{i1} phosphorylation on sarcomere disassembly.

A, Endogenous phospho-adducin patterns in neonatal mouse hearts: phospho-sites (T445/T480, S12/S355, S714/S724, S408/S436/S481) costained with sarcomeric proteins Tnnt2 or α -actinin. Arrows and arrowheads indicate colocalization with disassembled and assembled sarcomeres, respectively. **B**, NRVM showing Add1_{pT445} expression, stained with α -actinin (red) and pT445 (green), noting its translocation from the nucleus to the cytoplasm during mitosis. **C**, **Left**, Representative Western blot (WB). **Right**, Quantitative comparison of Add1_{pT445} endogenous expression in relative to Gapdh. Tnnt2 is used as an age indicator. **D**, Representative images of NRVM transduced with AAV6 viral particles for phospho-mimic or nonphospho-mimic T445/T480. **Top left**, Adducin mutants are expressed with 3 tandem FLAG epitopes at the N terminus. Cells were immunostained with α -actinin (red) to visualize sarcomere structure. Adducin mutants are detected by FLAG antibody (green). High-magnification images of representative region (insets) are shown on the **right**. Dotted lines were drawn around the cell border. **E**, Quantitative analysis of disassembled sarcomeres induced by adducin overexpression in **D**. **F**, Generation strategy for cardiac-specific Add1_{i1} phospho-transgenic mice. **G**, Hematoxylin and eosin staining of control and cardiac-specific Add1_{i1} phospho-transgenic. **H**, (Continued)

Figure 3 Continued. HW/BW in control and phospho-transgenic mice. **I**, Images showing phospho-Add1_{i2} expression patterns in transgenic mice at postnatal day 14 (P14) and P28, with **(bottom)** high-magnification views of selective phospho-adducin mimic overexpression cardiomyocytes. **J**, Proportion of cardiomyocytes expressing pAdd1 from **I**. **K**, Sarcomere patterns in phospho-Add1_{i1} transgenic mice at P14 and P28, with insets showing high-magnification images. Dotted lines are drawn around the outer and inner edges of cardiomyocytes. **L**, Quantitative analysis of sarcomere disassembly. Scale bar, 10 μ m (**A, B, D, I, and K**); 1 mm (**G**). Data are presented as mean \pm SD. Statistical analyses: Kruskal-Wallis with uncorrected Dunn test (**C**) or Mann-Whitney *U* test (2-tailed; **J**) or 2-way ANOVA with Tukey post hoc test (**E and L**); **P*<0.05, ***P*<0.01, ****P*<0.001, and *****P*<0.0001.

at 2 months (Figure 5C) compared with WT. Quantitative reverse-transcription polymerase chain reaction analysis confirmed increased expression levels of Add1_{i2} (Figure 5D), and immunostaining showed colocalization of Add1 and Add3 in p-dTG cardiomyocyte cytoplasm (Figure S7A). It is interesting that p-dTG cardiomyocytes displayed disassembled sarcomeres across developmental stages (P7, P14, P21, and 2 months), with more pronounced disassembly in early neonatal stages (Figure 5Ei through 5Eiv). In adult cardiomyocytes, partial disassembly was primarily observed around the nuclei and cell periphery, with complete clearance of sarcomeres in these zones. Furthermore, analysis of proliferation markers, including pH3 and aurora B kinase, indicated an increase in proliferative cardiomyocytes at P21 and 2 months (Figure S7B and S7C), without changes in cell size (Figure S7D) or nucleation (Figure S7E). These findings suggest that the concomitant expression of these proteins promotes persistent sarcomere disassembly and potentially cardiomyocyte proliferation.

Given the variations in transgene copy numbers or integration sites could affect protein overexpression, we verified and assessed the Add1_{i2} and Add3 expression in our TG lines using WB. All TG lines showed significantly higher transgene protein levels compared with WT littermates (Figure S8). The dTG line exhibited double the Add1_{i2} levels, likely because of reduced Add1 degradation from Add3 overexpression. However, Add1_{i2} levels were low in the p-dTG line, possibly because of the limited detection of phospho-mimic adducin protein of our antibody.

Identification of Irak4 as the Kinase Responsible for Adducin Phosphorylation in Cardiomyocytes

To understand the phosphorylation mechanism of Add1 at T445/T480, crucial for sarcomere disassembly, we conducted a kinase screening assay with 245 kinases. This initial screen revealed 7 kinases active on T445 (Figure 5F, left; Table S2). Peptide of T480 only showed a significant response to kinase Vrk1 (Figure 5F, right). We then performed a secondary screen on the top hits outlined above using a HitConfirmation dose-response assay. The result confirmed Nek1 (NIMA-related kinase 1), Irak4 (interleukin 1 receptor associated kinase 4), and doublecortin-like and CAM kinase-like 2 (Dcamkl2) as key kinases for T445 phosphorylation, with a less pro-

nounced effect on T480 (Figure 5G; Table S3). In P4 hearts, both Irak4 and Nek1 colocalized with disassembled sarcomeres (Figure 5H).

We then explored the role of Irak4 in inducing sarcomere disassembly. In vitro overexpression of Irak4 by AAV6 infection led to NRVMs sarcomere disassembly (Figure 5Ii), correlated with cytoplasmic phosphorylated Add1-pT445 (Figure 5Iii), whereas in Irak4-negative cells, Add1 remained nuclear. However, Nek1 overexpression in NRVMs showed no apparent effect on sarcomeres or adducin phosphorylation (data not shown). To assess sarcomere changes in vivo, we generated an AAV9-Irak4 virus. We injected this virus into neonatal mouse hearts at P1 and collected hearts at P15, a time point well beyond cell cycle exit of neonatal cardiomyocytes. Immunostaining on heart sections demonstrated that cardiomyocytes with Irak4 overexpression displayed prominent sarcomere disassembly (Figure 5J). These results indicate that Irak4 phosphorylates adducin in vitro and in vivo and induces sarcomere disassembly. Collectively, our results identify the adducin heterodimer as a key regulator in cardiomyocyte sarcomere disassembly during mitosis.

Identification of Binding Partners for the Adducin Complex During Regenerative and Nonregenerative Phases

Our findings suggest phosphorylated adducin heterodimers play a key role in cardiomyocyte sarcomere disassembly. To identify the binding partners of adducin in cardiomyocytes, we conducted Add1 Co-IP/MS analysis on protein extracts from P1 and P7MI hearts. This approach, similar to our previous Tnnt2 pulldown but using Add1 antibody as bait, revealed that Add1 shares many binding targets with Tnnt2 (Figure 6A; Table S4). This result suggests a significant interaction of Add1 with sarcomeric proteins in neonatal hearts.

Considering that adducin functions as an α/γ duplex, the aforementioned single antibody-based pulldown might not fully capture its binding pattern, especially given the limited adducin expression in adult hearts. To investigate why sarcomere disassembly is more pronounced in neonatal than in adult cardiomyocytes, including those in dTG hearts, we performed a pulldown study using a purified Add1/Add3 complex as bait with heart extracts from disassembly (P1) and nondisassembly (P21) stages. We cloned both Add1 and Add3 genes into the plasmid

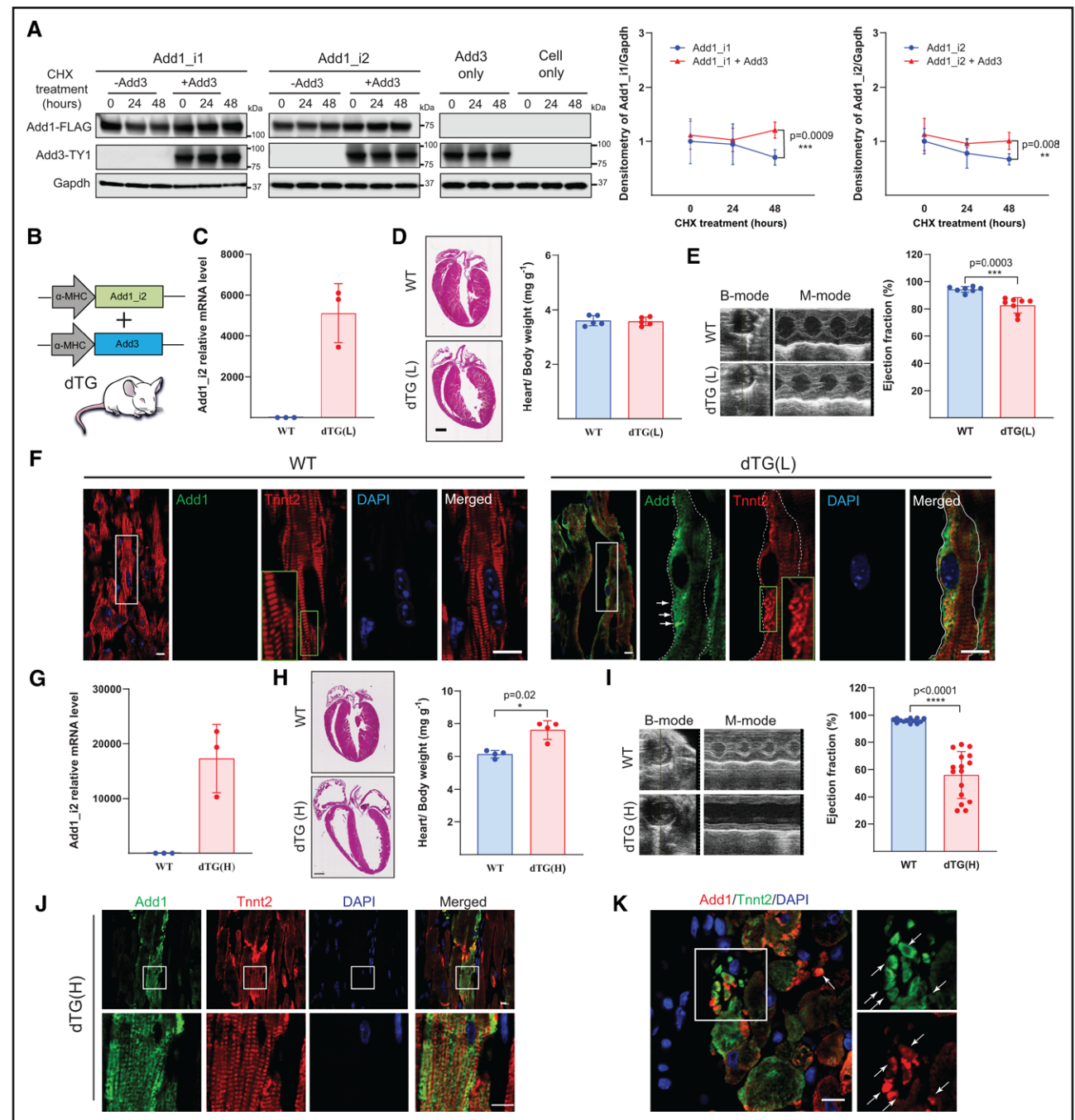


Figure 4. Coexpression of nonphosphorylated Add1_i2 with Add3 induces partial sarcomere disassembly.

A, HEK293T were transfected with *3xFLAG-Add1* variants, either with or without *3xTY1-Add3*, and treated with cycloheximide (CHX) to halt protein translation; cell collection at 0, 24, and 48 hours after treatment. **Left**, Representative Western blot (WB). **Right**, Assessment of relative protein levels of Add1_i1 and Add1_i2 (normalized FLAG to Gapdh) in the absence or presence of Add3. **B**, Generation strategy for cardiac-specific *Add1_i2/Add3* dTG mice. Both expression constructs were driven by an α -MHC promoter. **C**, Quantitative reverse-transcription polymerase chain reaction (qPCR) analysis of Add1_i2 mRNA in 2-month-old low expression dTG(L) hearts, normalized to wild-type (WT). **D, Left**, Hematoxylin and eosin (H&E) staining and **(right)** HW/BW comparison in 2-month-old dTG(L) mice. **E, Left**, Echocardiography and **(right)** left ventricular systolic function in 2-month-old dTG(L) mice. **F**, Sarcomere patterns in 2-month-old WT and dTG(L) hearts and high-magnification images of specific regions are provided. The dotted lines indicate cardiomyocyte borders, with green insets highlighting partially disassembled sarcomeres. Arrows indicate corresponding adducin expression. **G**, qPCR analysis of Add1_i2 mRNA in 2-month-old low expression dTG(H) hearts, normalized to WT. **H, Left**, H&E staining and HW/BW comparison **(right)** in 2-month-old dTG(H) mice. **I, Left**, Echocardiography and left ventricular systolic function **(right)** in 1-month-old dTG(H) mice. **J, Top**, Sarcomere pattern in 1-month-old dTG(H) hearts with robust disassembly. **Bottom**, High-magnification images of specific regions show the regions with a lack of disassembly. **K, Left**, Evidence of cardiomyocyte fragmentation and high magnification **(right)** of the inset indicate colocalization of Add1 and Tnnt2 in fragmented sarcomere (arrows). Scale bar=10 μ m (**F, J, and K**); 1 mm (**D and H**). Data are presented as mean \pm SD. Statistical analyses: repeated-measures 2-way ANOVA with Tukey post hoc test (**A**) or Mann-Whitney *U* test (2-tailed; **C, E, and G** through **I**) were used to determine statistical significance; * P <0.05, ** P <0.01, *** P <0.001, and **** P <0.0001.

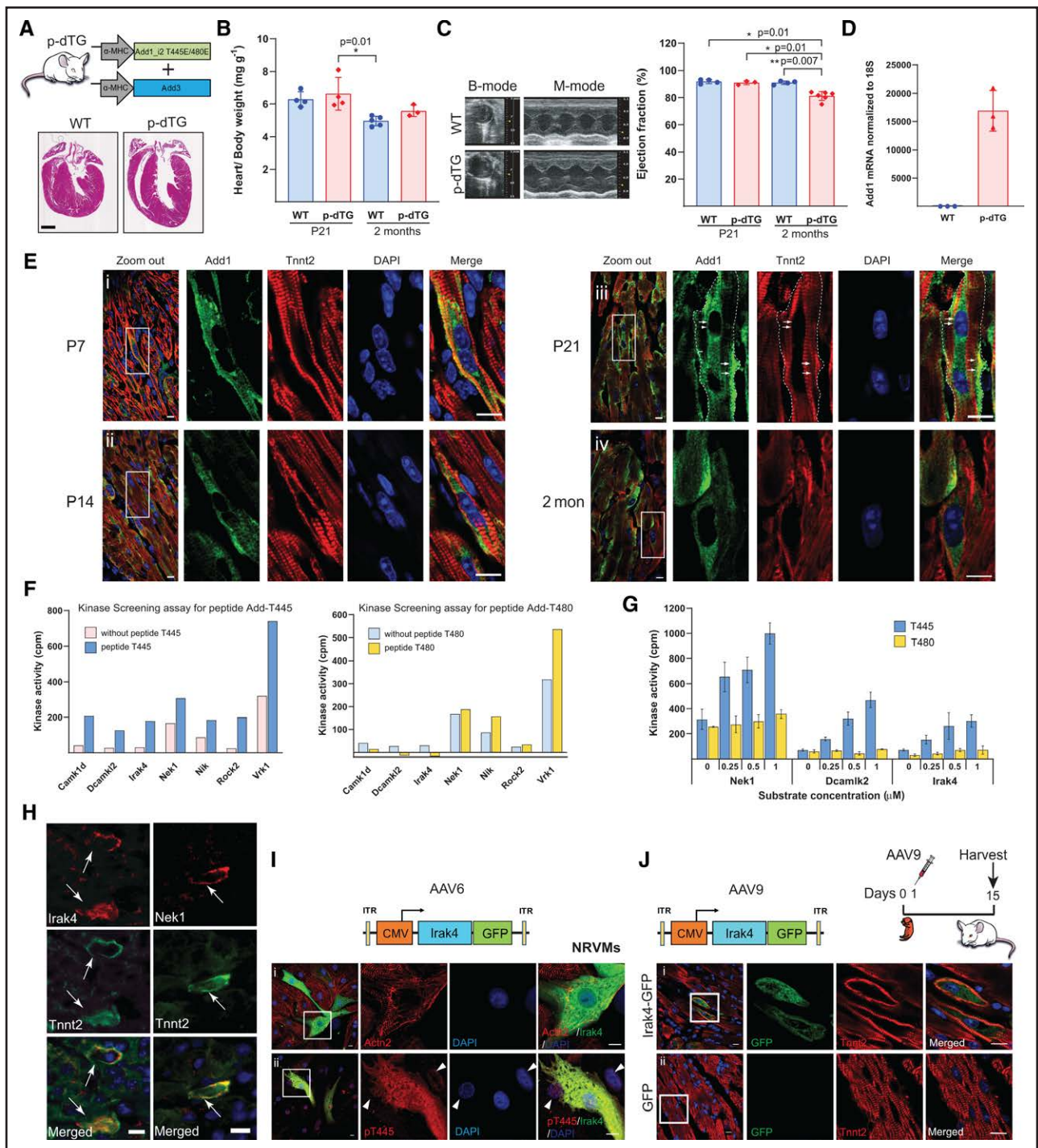


Figure 5. Coexpression of phospho-mimic Add1_{i2} with Add3 promotes sarcomere disassembly.

A, Top, Schematic strategy for generating cardiac-specific phospho-mimic Add1_{i2}/Add3 double transgenic mice (p-dTG), with T445 and T480 glutamic acid (Glu) substitutions in Add1_{i2} to mimic phosphorylation, driven by an α -MHC promoter. **Bottom**, Hematoxylin and eosin staining of 2-month-old control and p-dTG hearts. **B**, HW/BW in wild-type (WT) and p-dTG mice in postnatal day 21 (P21) and 2-month-old mice. **C**, **Left**, Echocardiography and **(right)** left ventricular systolic function in P21 and 2-month-old p-dTG mice. **D**, Quantitative reverse-transcription polymerase chain reaction results for Add1_{i2} in 2-month-old p-dTG. **E**, Sarcomere structure in p-dTG hearts at P7 (**i**), P14 (**ii**), P21 (**iii**), and 2 months (**iv**). High-magnification images of selected regions show sarcomere absence in areas with high adducin expression (arrows). Dotted lines outline cardiomyocyte borders. **F**, Identification of 7 kinase candidates potentially phosphorylating T445 (**left**) and T480 (**right**) using 245 Ser/Thr peptide kinase assays, with corrected kinase activity values depicted. **G**, Verification of Nek1, Dcam1, and Irak4 kinase activity in phosphorylating T445 and T480 using serine/threonine kinase dose-response assays. Each kinase was tested at 3 concentrations in triplicate. **H**, Endogenous expression pattern of **(left)** Irak4 and **(right)** Nek1 in the regenerating neonatal heart, with positive signals indicated (arrows). **I**, **Top**, Schematic of Irak4 expression in AAV6 constructs. Irak4 (green) overexpression in NRVMs causes sarcomere disassembly (stained with α -actinin, red) disassembly (**i**) and translocation of Add1_{pT445} (red) from nucleus to cytoplasm (**ii**). Arrowheads indicate adducin (*Continued*)

Figure 5 Continued. is expressed in the nuclei in Irak4-negative cells. **J, Top left**, Schematic of Irak4 expression in AAV9 constructs. **Top right**, Experimental design for neonatal AAV injection. **Bottom**, Results after AAV9-Irak4-GFP injection in CD1 pups at P1, showing intense sarcomere disassembly in cardiomyocytes compared to littermate controls at P15. Scale bar=10 μm (**E** and **H** through **J**); scale bar=1 mm (**A**). Data are presented as mean \pm SD. Statistical analyses: 2-way ANOVA with Bonferroni multiple comparisons test (**B** and **C**), Mann-Whitney *U* test (2-tailed; **D**); * P <0.05, ** P <0.01, *** P <0.001, and **** P <0.0001.

pETDuet, which coexpresses 2 open reading frames together and forms a duplex naturally in cells, generating long (Add1_i1/Add3) and short (Add1_i2/Add3) forms (Figure 6B). After incubating these purified duplexes with heart lysates and binding them to Ni-NTA beads, we analyzed bound proteins using mass spectrometry (Figure 6C). We also included a negative control where heart lysates were mixed with Ni-NTA beads. Log₂(sample/control) fold changes >1.5 were considered for further Ingenuity Pathway Analysis. Figure 6D is a bar graph of statistically significant canonical pathways enriched in the sample. Interestingly, the only pathway upregulated at P1 compared with P21 was the actin cytoskeleton signaling.

Network plots showed how proteins of this pathway interact with long or short adducins at different stages (Figure 6E). It is interesting that both adducin long and short forms specifically interacted with certain sarcomeric proteins, such as α -actinin at P1, but not P21. In adult cardiomyocytes, α -actinin is localized to the Z-disks, in which it is critical for organizing sarcomere structure. This finding suggested that adducin and α -actinin interaction could be key for sarcomere disassembly during the cardiomyocyte proliferation phase. Therefore, we further explore their interaction by using proximity ligation assay (PLA) with an anti-Add1_pT445 antibody in neonatal hearts, using Tnnt2 binding to α -actinin as a positive control. The results revealed a strong association of Add1_pT445 with α -actinin at this stage (Figure 6F). Furthermore, using Immunogold electron microscopy, we examined Add_pT445 subcellular localization in neonatal cardiomyocytes, finding it at the Z-disks of sarcomeres (Figure 6Gi), where α -actinin is also located, and also associated with disassembled sarcomeres near the cellular cortex (Figure 6Gii). Considering the role of adducin in sarcomere disassembly and its association to α -actinin, we hypothesized that this interaction might extract α -actinin from sarcomeres, leading to disassembly. To investigate whether the loss of α -actinin could promote disassembly, we developed an ACTN2-deficient human induced pluripotent stem cell cardiomyocyte line using clustered regularly interspaced short palindromic repeats (CRISPR)/Cas9 (CRISPR-associated protein 9), leading to an expected ACTN2 frameshift. WB analysis confirmed the effective deletion of ACTN2 (Figure S9A). Remarkably, after differentiation to cardiomyocytes, these cells exhibited a sarcomere disassembly phenotype similar to adducin transgenics, with actin mainly localizing to the cellular cortex (Figure S9B). These insights provide a deeper understanding of the

molecular interactions and localization between adducin and α -actinin in relation to sarcomere disassembly during neonatal cardiomyocyte mitosis.

DISCUSSION

Numerous published reports have outlined various mechanisms of cardiomyocyte cell cycle regulation in recent years. These mechanisms encompass diverse pathways including direct cell cycle regulators, transcription factors, micro-RNAs, Lnc-RNAs, and nonmyocyte factors including extracellular matrix, immunological, and environmental factors among others. However, striated muscle-specific mechanisms that regulate sarcomere organization during cardiomyocyte mitosis remain poorly understood. In the current report, we demonstrate that the cytoskeleton protein adducin regulates sarcomere disassembly during cardiomyocyte mitosis. In noncontractile cells, previous studies have identified mechanisms that regulate cytoskeletal assembly and actin sheets dimerization. For example, the cytoskeletal regulatory protein adducin is a major regulator of actin bundling and actin-spectrin interaction.^{38,39} The adducin family is composed of 3 members, namely α -, β -, or γ -adducins. The fully assembled adducin is composed of heterodimers of homologous α and β or γ subunits. Despite the known role of adducin in actin assembly in noncontractile cells, its role in contractile cells is entirely unknown.

Our results stem from a proteomics screen of proteins that differentially associate with Tnnt2 during an early regenerative time point of the newborn mouse heart. Although several cytoskeleton proteins appeared to be differentially associated with Tnnt2 during this early time point, we focused on adducin given its known cytoskeleton regulatory role in noncontractile cells. We provide several lines of evidence that support the association of adducin with sarcomeric proteins. First, immunostaining demonstrates that α -adducin is localized to the cytoplasm and membrane only in cardiomyocytes with disassembled sarcomeres. Second, Co-IP using Add1 antibody or purified α/γ -adducin complex suggests a possible association of adducin with sarcomeric proteins, in particular α -actinin. Third, we identified a membrane-associated phospho-isoform of Add1, which binds α -actinin by PLA, and colocalizes with membrane-associated sarcomeres by Immunogold electron microscopy labeled with nanogold particles. These results indicate that Add1 is a sarcomere-associated cytoskeletal protein in cardiomyocytes.

It is important to note that gain-of-function studies in vitro and in vivo demonstrate that forced adducin expression

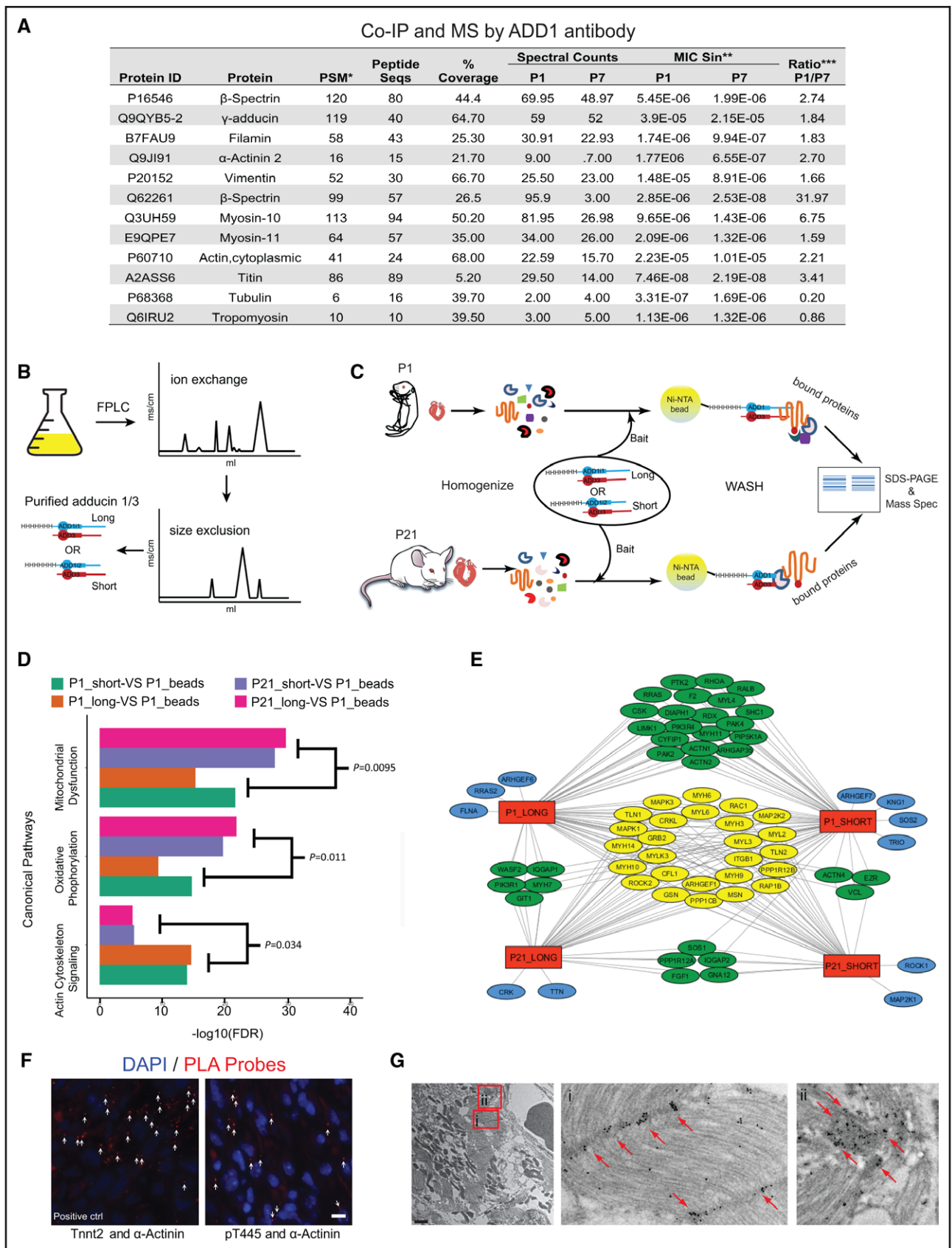


Figure 6. Analysis of coimmunoprecipitation (Co-IP)/mass spectrometry (MS) with purified adducin complex.

A, The table enumerates key proteins associated with Add1, as identified through Co-IP/MS, with a similar strategy as Figure 1C. **B**, Schematic of the purification process of short and long adducin complexes. **C**, Schematic of Co-IP/MS by purified adducin complex pulldown. (Continued)

Figure 6 Continued. **D**, Bar graph for Canonical Pathways enriched in each sample. FDR, false discovery rate. **E**, Network plot of cytoskeleton proteins from the pull-down assay interact with adducin long or adducin short isoforms at different regenerative time points (postnatal day [P1] and P21). Different color labels indicate common and unique proteins among sample groups (red, all sample groups; yellow, common to all groups; green, common to 2 or 3 groups; blue, unique to each group). **F**, PLA result shows the direct interaction between Add1_pT445 and α -actinin in P4 heart tissue. Red dots (arrows) represent fluorescent signals of close interactions. Interaction between α -actinin and Tntt2 serves as a positive control. **G**, Immunogold electron microscopy image details the subcellular location of Add1_pT445 in cardiomyocytes with disassembled sarcomeres in neonatal P1MI hearts. Two red boxes are magnified in the right 2 panels showing Add1_pT445 at Z-disks (**i**) and at Z-disks associated with the plasma membrane in cardiomyocytes with disassembled sarcomeres (**ii**). Red arrows indicate the location of adducin. Scale bar=1 μ m (**G**); scale bar=10 μ m (**F**).

induces sarcomere disassembly. We show that expression of several isoforms of adducin induces sarcomere disassembly in primary neonatal cardiomyocytes in culture. In addition, both single TG Add1_i2 and Add1_i1 phosphomimic manifest a nonhomogeneous expression pattern of adducin that resulted in extension of the sarcomere disassembly window until P14, but not adulthood. Protein stability assays demonstrated that coexpression of Add1 or Add3 is necessary for the stability of both proteins, and this was confirmed in vivo in the dTG lines that displayed stable expression of both Add1 and Add3 through adulthood. We also demonstrate that although the nonphospho-mimic dTG lines display persistent adducin expression, this did not result in pronounced sarcomere disassembly even at high expression levels, whereas the same dTG construct with a constitutively active T445/T480 phospho-mimic resulted in sarcomere disassembly that persisted to adulthood.

One important limitation of the current findings is the incomplete disassembly we observed in adult cardiomyocytes even in the phospho-mimic dTG. Although we noted complete disassembly in the early postnatal period, most adult cardiomyocytes displayed incomplete disassembly that appeared to be localized to the zone surrounding nuclei and in the periphery of cardiomyocytes with complete clearance of the sarcomeres in these zones. This incomplete disassembly likely explains the lack of severe decline in LV systolic function in this dTG line. The mechanism of this differential effect of adducin on early postnatal compared with adult sarcomeres is unclear but might be related to changes in sarcomere phenotype with age. To address this question, we used purified α (either short or long isoform)- γ adducin protein complex to identify binding partners in early neonatal and adolescent hearts. The results demonstrate that the adducin complex differentially binds to cytoskeletal proteins depending on the postnatal age. Specifically, both short and long forms of the adducin complex appear to bind selectively to the cardiac-specific α -actinin in P1 but not P21 hearts. PLA and Immunogold electron microscopy support the notion that adducin associates with α -actinin in Z-disks. Although adducin has not been previously shown to bind α -actinin, α -actinin belongs to the spectrin superfamily, and spectrin is a known binding partner of adducin in noncontractile cells. Given the known role of α -actinin in anchoring actin to Z-disks in cardiomyocytes, future studies should explore the potential role of α -actinin in

the regulation of sarcomere disassembly downstream of adducin. Collectively, these results identify an important regulatory mechanism of sarcomere disassembly that links cytoskeleton organization to cell cycle regulation in mammalian cardiomyocytes and provides insights into the challenges of mitosis in actively contractile cells.

ARTICLE INFORMATION

Received January 8, 2022; accepted March 29, 2024.

Affiliations

Departments of Internal Medicine (Cardiology) (FX, N.U.N.N., P.W., S.L., C.-C.H., S.T., W.K., X.L., N.T.L., I.M.-M., W.E., A.C.C., A.H.M.P., J.A.H., H.A.S.), Eugene McDermott Center for Human Growth and Development (M.K., C.X.), Lyda Hill Department of Bioinformatics (C.X.), O'Donnell School of Public Health (C.X.), Moss Heart Center (J.A.H.), Department of Molecular Biology (J.A.H., H.A.S.), Department of Biophysics (H.A.S.), Hamon Center for Regenerative Science and Medicine (H.A.S.), University of Texas Southwestern Medical Center, Dallas. Life Science Center, Tsukuba Advanced Research Alliance, University of Tsukuba, Japan (W.K.). Biosciences National Laboratory, Brazilian Center for Research in Energy and Materials, Campinas (A.C.C., A.H.M.P.). Center for Cardiovascular Research, Division of Cardiovascular Health and Disease, Department of Internal Medicine, University of Cincinnati College of Medicine, OH (R.S., S.S.). Amgen Research, Department of Cardiometabolic Disorders, Amgen, South San Francisco, CA (R.S.). University of Connecticut Health Center, Farmington (F.A.L., J.T.H.). Jackson Laboratory for Genomic Medicine, Farmington, CT (J.T.H.). Gene & Cell Therapy Institute, Mass General Brigham, Cambridge, MA (R.J.H.). Centro Nacional de Investigaciones Cardiovasculares, Madrid, Spain (H.A.S.).

Acknowledgments

The authors gratefully acknowledge the Molecular Pathology Core and J. Shelton for histology support; McDermott Center Sequencing and Bioinformatics Cores for sequencing and analysis; H. Mirzaei, D.C. Trudgian, and A. Lemoff for MS analysis; K. Luby-Phelps and A. Darehshouri for electron microscopy support; and R.E. Hammer, J. Ritter, M. Nguyen, and H. Zhu for microinjection assistance.

Sources of Funding

This work was supported by grants from the National Institutes of Health (R01_HL137415, R01_HL147276, R01_HL1491371, P01_HL160476-01A1, R35_HL166563-01, P01_HL160488 [H.A.S.]; R01_HL128215, R01_HL147933, R01_HL155765, R01_HL164586 [J.A.H.]; R01_HL105826, R01_AR078001, R38_HL155775 [S.S.]; R01_HL165220, and R01_HL142787 [J.T.S.]); the American Heart Association (AHA_856552, AHA_19POST34450039 [N.U.N.N.]; AHA_903385 [I.M.M.]; AHA_SURF_25UFEL34380251, and AHA_TPA_945748 [S.S.]); the Leducq Transatlantic Network of Excellence (H.A.S.); the Hamon Center for Regenerative Science and Medicine (H.A.S.); and an Amgen Post-Doctoral fellowship (R.S.).

Disclosures

S.S. provides consulting and collaborative research studies to the Leducq Foundation (CURE-PLAN), Red Saree Inc, Alexion, and Affinia Therapeutics Inc, but such work is unrelated to the content of this article. The other authors report no conflicts.

Supplemental Material

Expanded Methods
Figures S1–S9
Tables S1–S5
Excel Files S1–S4

REFERENCES

- Bui AL, Horwich TB, Fonarow GC. Epidemiology and risk profile of heart failure. *Nat Rev Cardiol*. 2011;8:30–41. doi: 10.1038/nrcardio.2010.165
- Bergmann O, Zdunek S, Frisen J, Bernard S, Druid H, Jovinge S. Cardiomyocyte renewal in humans. *Circ Res*. 2012;110:e17–e18; author reply e19. doi: 10.1161/CIRCRESAHA.111.259598
- Laflamme MA, Myerson D, Saffitz JE, Murry CE. Evidence for cardiomyocyte repopulation by extracardiac progenitors in transplanted human hearts. *Circ Res*. 2002;90:634–640. doi: 10.1161/01.res.0000014822.62629.eb
- Bergmann O, Bhardwaj RD, Bernard S, Zdunek S, Barnabe-Heider F, Walsh S, Zupicic J, Alkass K, Buchholz BA, Druid H, et al. Evidence for cardiomyocyte renewal in humans. *Science*. 2009;324:98–102. doi: 10.1126/science.1164680
- Nadal-Ginard B. [Generation of new cardiomyocytes in the adult heart: prospects of myocardial regeneration as an alternative to cardiac transplantation]. *Rev Esp Cardiol*. 2001;54:543–550. doi: 10.1016/s0300-8932(01)76354-3
- Quaini F, Urbanek K, Beltrami AP, Finato N, Beltrami CA, Nadal-Ginard B, Kajstura J, Leri A, Anversa P. Chimerism of the transplanted heart. *N Engl J Med*. 2002;346:5–15. doi: 10.1056/NEJMoa012081
- Hsieh PC, Segers VF, Davis ME, MacGillivray C, Gannon J, Molkentin JD, Robbins J, Lee RT. Evidence from a genetic fate-mapping study that stem cells refresh adult mammalian cardiomyocytes after injury. *Nat Med*. 2007;13:970–974. doi: 10.1038/nm1618
- Becker RO, Chapin S, Sherry R. Regeneration of the ventricular myocardium in amphibians. *Nature*. 1974;248:145–147. doi: 10.1038/248145a0
- Oberpriller JO, Oberpriller JC. Response of the adult newt ventricle to injury. *J Exp Zool*. 1974;187:249–253. doi: 10.1002/jez.1401870208
- Neff AW, Dent AE, Armstrong JB. Heart development and regeneration in urodeles. *Int J Dev Biol*. 1996;40:719–725.
- Flink IL. Cell cycle reentry of ventricular and atrial cardiomyocytes and cells within the epicardium following amputation of the ventricular apex in the axolotl, *Amblystoma mexicanum*: confocal microscopic immunofluorescent image analysis of bromodeoxyuridine-labeled nuclei. *Anat Embryol*. 2002;205:235–244. doi: 10.1007/s00429-002-0249-6
- Poss KD, Wilson LG, Keating MT. Heart regeneration in zebrafish. *Science*. 2002;298:2188–2190. doi: 10.1126/science.1077857
- Wang J, Panakova D, Kikuchi K, Holdway JE, Gemberling M, Burris JS, Singh SP, Dickson AL, Lin YF, Sabeh MK, et al. The regenerative capacity of zebrafish reverses cardiac failure caused by genetic cardiomyocyte depletion. *Development*. 2011;138:3421–3430. doi: 10.1242/dev.068601
- Gonzalez-Rosa JM, Martin V, Peralta M, Torres M, Mercader N. Extensive scar formation and regression during heart regeneration after cryoinjury in zebrafish. *Development*. 2011;138:1663–1674. doi: 10.1242/dev.060897
- Porrello ER, Mahmoud AI, Simpson E, Hill JA, Richardson JA, Olson EN, Sadek HA. Transient regenerative potential of the neonatal mouse heart. *Science*. 2011;331:1078–1080. doi: 10.1126/science.1200708
- Porrello ER, Mahmoud AI, Simpson E, Johnson BA, Grinsfelder D, Canseco D, Mammen PP, Rothermel BA, Olson EN, Sadek HA. Regulation of neonatal and adult mammalian heart regeneration by the miR-15 family. *Proc Natl Acad Sci USA*. 2013;110:187–192. doi: 10.1073/pnas.1208863110
- Mahmoud AI, Kocabas F, Muralidhar SA, Kimura W, Koura AS, Thet S, Porrello ER, Sadek HA. Meis1 regulates postnatal cardiomyocyte cell cycle arrest. *Nature*. 2013;497:249–253. doi: 10.1038/nature12054
- Sdek P, Zhao F, Wang Y, Huang CJ, Ko CY, Butler PC, Weiss JN, MacLellan WR. Rb and p130 control cell cycle gene silencing to maintain the postmitotic phenotype in cardiac myocytes. *J Cell Biol*. 2011;194:407–423. doi: 10.1083/jcb.201012049
- Xin M, Kim Y, Sutherland LB, Murakami M, Qi X, McAnally J, Porrello ER, Mahmoud AI, Tan W, Shelton JM, et al. Hippo pathway effector Yap promotes cardiac regeneration. *Proc Natl Acad Sci USA*. 2013;110:13839–13844. doi: 10.1073/pnas.1313192110
- Chen J, Huang ZP, Seok HY, Ding J, Kataoka M, Zhang Z, Hu X, Wang G, Lin Z, Wang S, et al. mir-17-92 cluster is required for and sufficient to induce cardiomyocyte proliferation in postnatal and adult hearts. *Circ Res*. 2013;112:1557–1566. doi: 10.1161/CIRCRESAHA.112.300658
- Eulalio A, Mano M, Dal Ferro M, Zentilin L, Sinagra G, Zacchigna S, Giacca M. Functional screening identifies miRNAs inducing cardiac regeneration. *Nature*. 2012;492:376–381. doi: 10.1038/nature11739
- Bersell K, Arab S, Haring B, Kuhn B. Neuregulin1/ErbB4 signaling induces cardiomyocyte proliferation and repair of heart injury. *Cell*. 2009;138:257–270. doi: 10.1016/j.cell.2009.04.060
- Porrello ER, Johnson BA, Aurora AB, Simpson E, Nam YJ, Matkovich SJ, Dorn GW 2nd, van Rooij E, Olson EN. MiR-15 family regulates postnatal mitotic arrest of cardiomyocytes. *Circ Res*. 2011;109:670–679. doi: 10.1161/CIRCRESAHA.111.248880
- Gerdes AM. *Cardiomyocyte Ultrastructure*. 2012.
- Jopling C, Sleep E, Raya M, Marti M, Raya A, Izpisua Belmonte JC. Zebrafish heart regeneration occurs by cardiomyocyte dedifferentiation and proliferation. *Nature*. 2010;464:606–609. doi: 10.1038/nature08899
- Kubin T, Poling J, Kostin S, Gajawada P, Hein S, Rees W, Wietelmann A, Tanaka M, Lorchner H, Schimanski S, et al. Oncostatin M is a major mediator of cardiomyocyte dedifferentiation and remodeling. *Cell Stem Cell*. 2011;9:420–432. doi: 10.1016/j.stem.2011.08.013
- Ahuja P, Perriard E, Perriard JC, Ehler E. Sequential myofibrillar breakdown accompanies mitotic division of mammalian cardiomyocytes. *J Cell Sci*. 2004;117:3295–3306. doi: 10.1242/jcs.01159
- Puente BN, Kimura W, Muralidhar SA, Moon J, Amatrua JF, Phelps KL, Grinsfelder D, Rothermel BA, Chen R, Garcia JA, et al. The oxygen-rich postnatal environment induces cardiomyocyte cell-cycle arrest through DNA damage response. *Cell*. 2014;157:565–579. doi: 10.1016/j.cell.2014.03.032
- Guo W, Schafer S, Greaser ML, Radke MH, Liss M, Govindarajan T, Maatz H, Schulz H, Li S, Parrish AM, et al. RBM20, a gene for hereditary cardiomyopathy, regulates titin splicing. *Nat Med*. 2012;18:766–773. doi: 10.1038/nm.2693
- Yang J, Hung LH, Licht T, Kostin S, Looso M, Khrameeva E, Bindereif A, Schneider A, Braun T. RBM24 is a major regulator of muscle-specific alternative splicing. *Dev Cell*. 2014;31:87–99. doi: 10.1016/j.devcel.2014.08.025
- Giudice J, Xia Z, Wang ET, Scavuzzo MA, Ward AJ, Kalsotra A, Wang W, Wehrens XH, Burge CB, Li W, et al. Alternative splicing regulates vesicular trafficking genes in cardiomyocytes during postnatal heart development. *Nat Commun*. 2014;5:3603. doi: 10.1038/ncomms4603
- Kong SW, Hu YW, Ho JW, Ikeda S, Polster S, John R, Hall JL, Bisping E, Pieske B, dos Remedios CG, et al. Heart failure-associated changes in RNA splicing of sarcomere genes. *Circ Cardiovasc Genet*. 2010;3:138–146. doi: 10.1161/CIRCGENETICS.109.904698
- Yin Z, Ren J, Guo W. Sarcomeric protein isoform transitions in cardiac muscle: a journey to heart failure. *Biochim Biophys Acta*. 2015;1852:47–52. doi: 10.1016/j.bbdis.2014.11.003
- Fukata Y, Oshiro N, Kinoshita N, Kawano Y, Matsuoka Y, Bennett V, Matsuura Y, Kaibuchi K. Phosphorylation of adducin by Rho-kinase plays a crucial role in cell motility. *J Cell Biol*. 1999;145:347–361. doi: 10.1083/jcb.145.2.347
- Chan PC, Hsu RY, Liu CW, Lai CC, Chen HC. Adducin-1 is essential for mitotic spindle assembly through its interaction with myosin-X. *J Cell Biol*. 2014;204:19–28. doi: 10.1083/jcb.201306083
- Matsuoka Y, Li X, Bennett V. Adducin is an in vivo substrate for protein kinase C: phosphorylation in the MARCKS-related domain inhibits activity in promoting spectrin-actin complexes and occurs in many cells, including dendritic spines of neurons. *J Cell Biol*. 1998;142:485–497. doi: 10.1083/jcb.142.2.485
- Matsuoka Y, Hughes CA, Bennett V. Adducin regulation. Definition of the calmodulin-binding domain and sites of phosphorylation by protein kinases A and C. *J Biol Chem*. 1996;271:25157–25166. doi: 10.1074/jbc.271.41.25157
- Bennett V, Lorenzo DN. Spectrin- and ankyrin-based membrane domains and the evolution of vertebrates. *Curr Top Membr*. 2013;72:1–37. doi: 10.1016/B978-0-12-417027-8.00001-5
- Franco T, Low PS. Erythrocyte adducin: a structural regulator of the red blood cell membrane. *Transf Clin Biol*. 2010;17:87–94. doi: 10.1016/j.tracli.2010.05.008